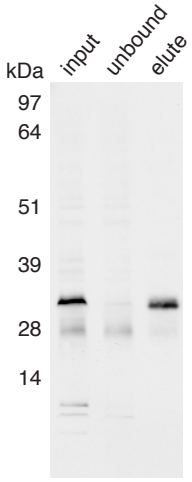

Supplementary Figure 1. Western blot detecting FLAG-labeled Rpb3 of immunoprecipitation samples of input lysate, unbound lysate and eluted protein. See Supplementary Methods for details.

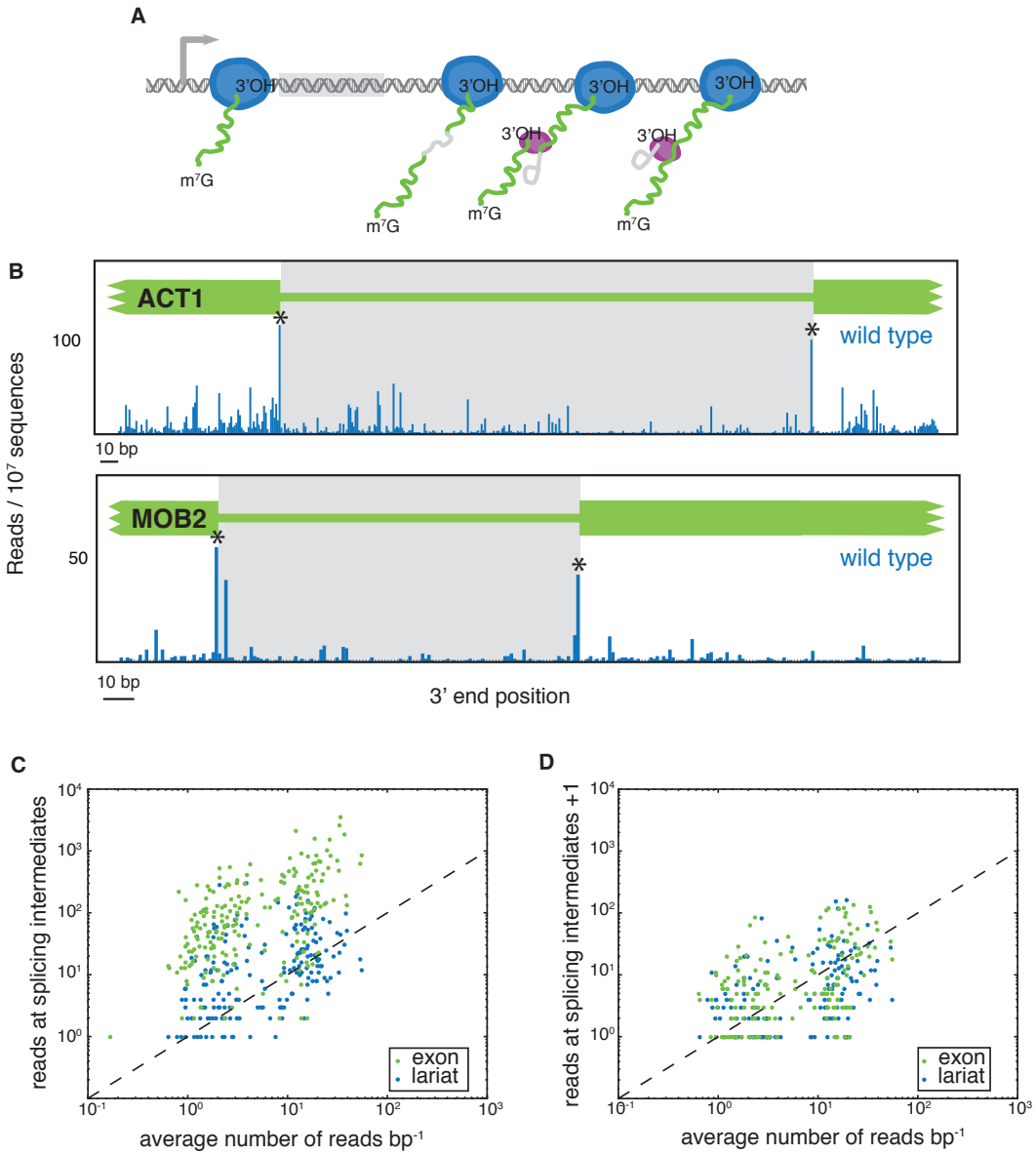

Supplementary Figure 2. Evidence of co-transcriptional splicing in yeast. **a,** A schematic showing how co-transcriptional splicing intermediates (e.g. spliced exon and excised lariat (grey)) would remain bound to RNAP II via the spliceosome (purple circle). **b,** Read densities for two spliced genes, *ACT1* and *MOB2*. Note the high densities at their precise exon-intron junctions indicated by stars. Average number of reads per base pair for spliced genes versus the gene's reads at the 3' end of splice junctions **(c)** and one base pair downstream from splice junctions **(d)**.

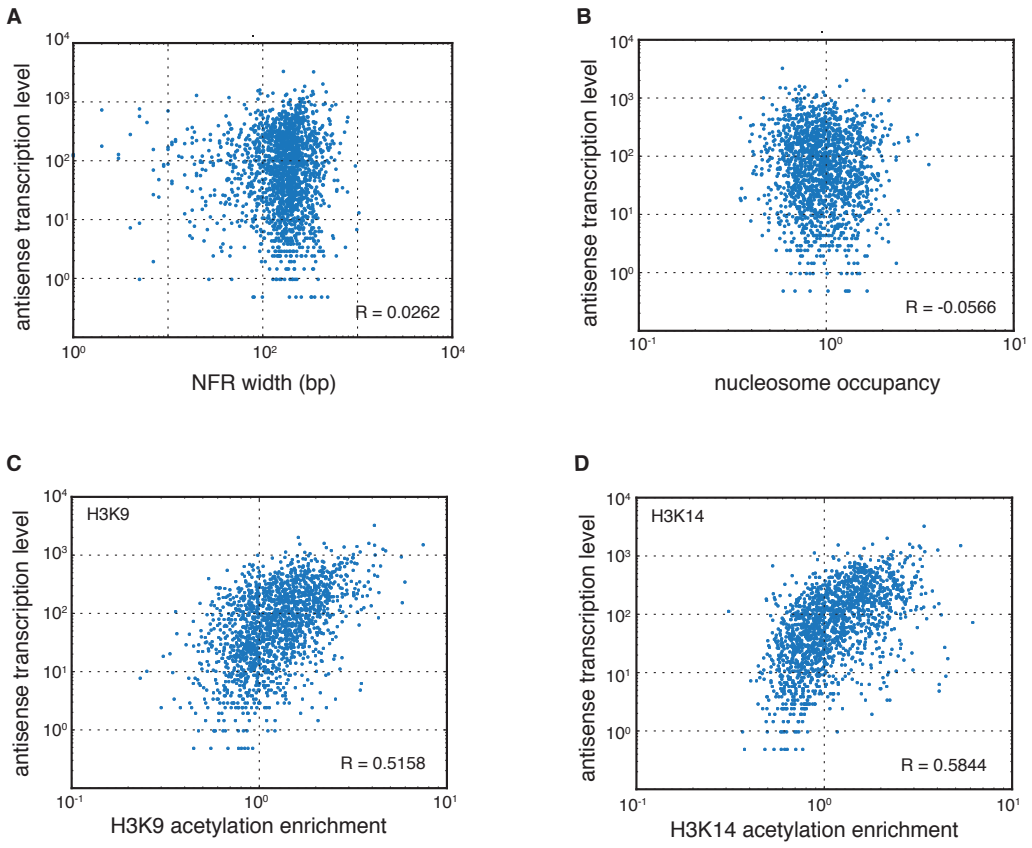

Supplementary Figure 3. Antisense transcription correlations. **a-b)** Antisense transcription level versus the width of the promoter's nucleosome free region (NFR) and nucleosome occupancy from available data [2]. R values are Spearman correlation coefficients. **c-d)** Antisense transcription level versus H3 acetylation enrichment from available data[1].

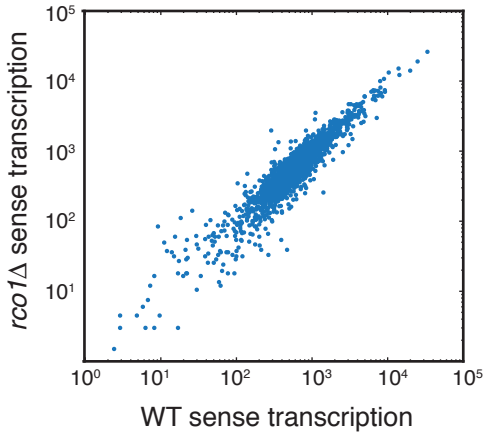

Supplementary Figure 4. Comparison between sense transcription in wild type strain and the *rco1Δ* strain at divergent promoters. R = 0.965, Pearson correlation coefficient. R = 0.914, Spearman correlation coefficient

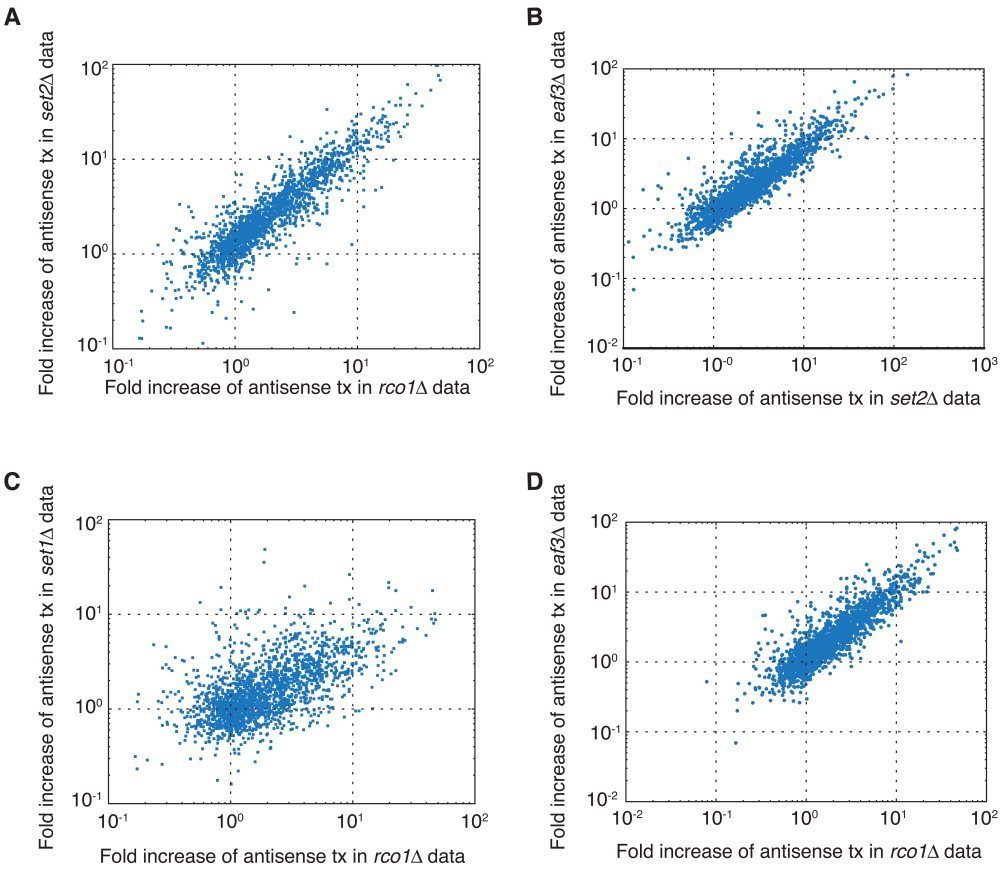

Supplementary Figure 5. Comparison of fold increases of antisense transcription (tx) in mutant strains compared to that in wild type.

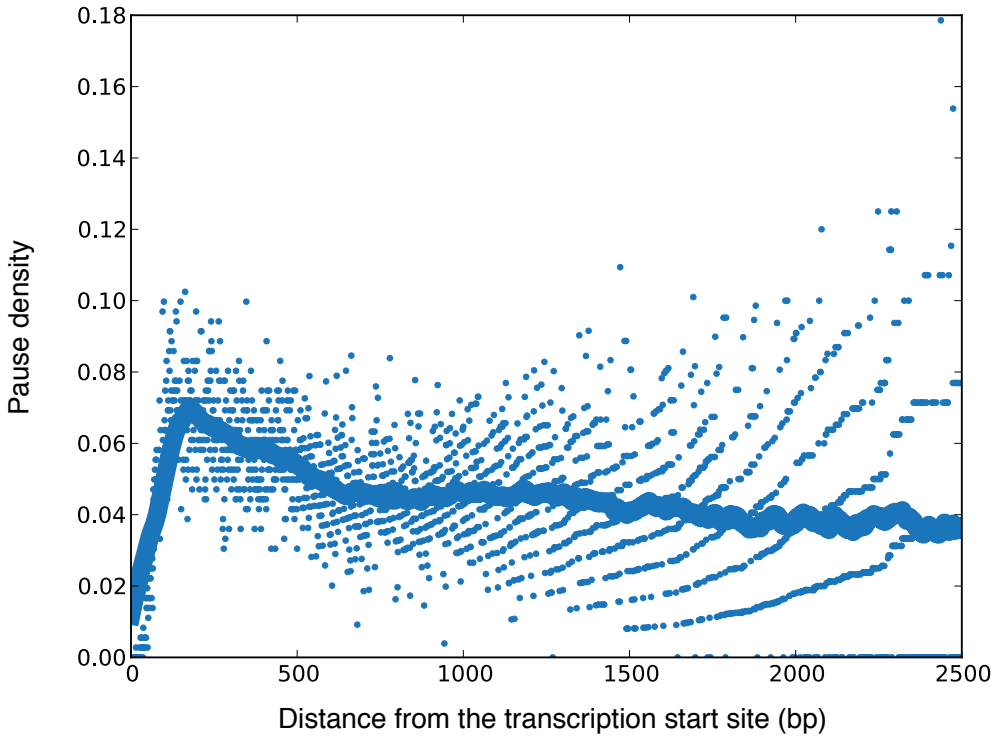

Supplementary Figure 6. Average pause density across gene bodies for highly expressed genes (N = 361, >4 reads/bp).

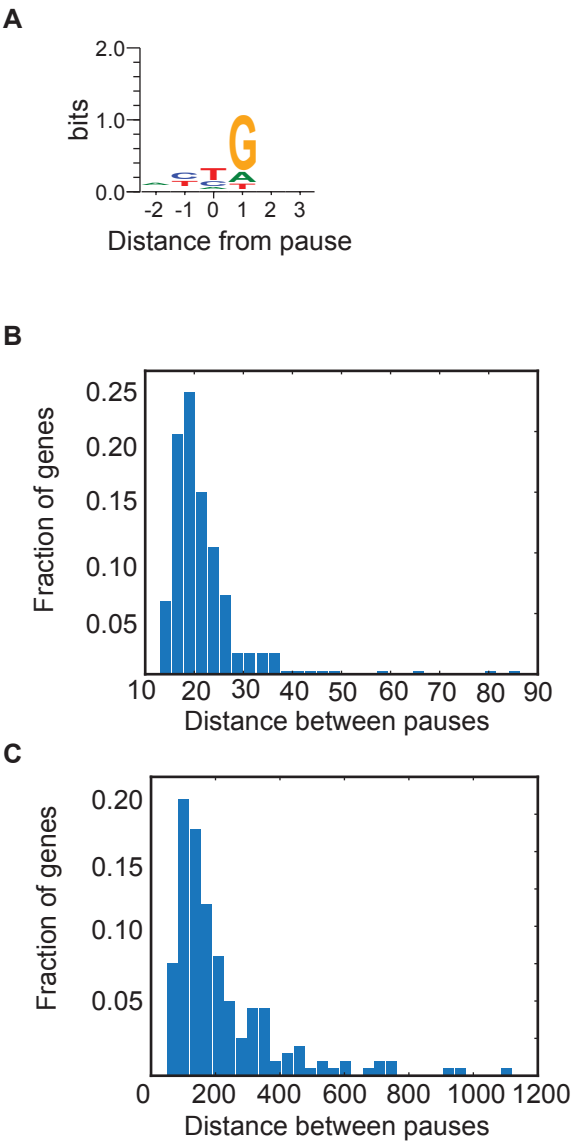

Supplementary Figure 7 Pause finding analysis on mRNA data **a)** Sequence consensus of extracted pauses in mRNA data shows a strong propensity for G's to occur at the base following the 3' end of the fragmented transcript. This bias occurred during the fragmentation of full length mRNA. After removing all pauses that are followed by a G, the average distance between pauses was measured for each gene for nascent RNA **(b)** and for fragmented mRNA **(c)**.

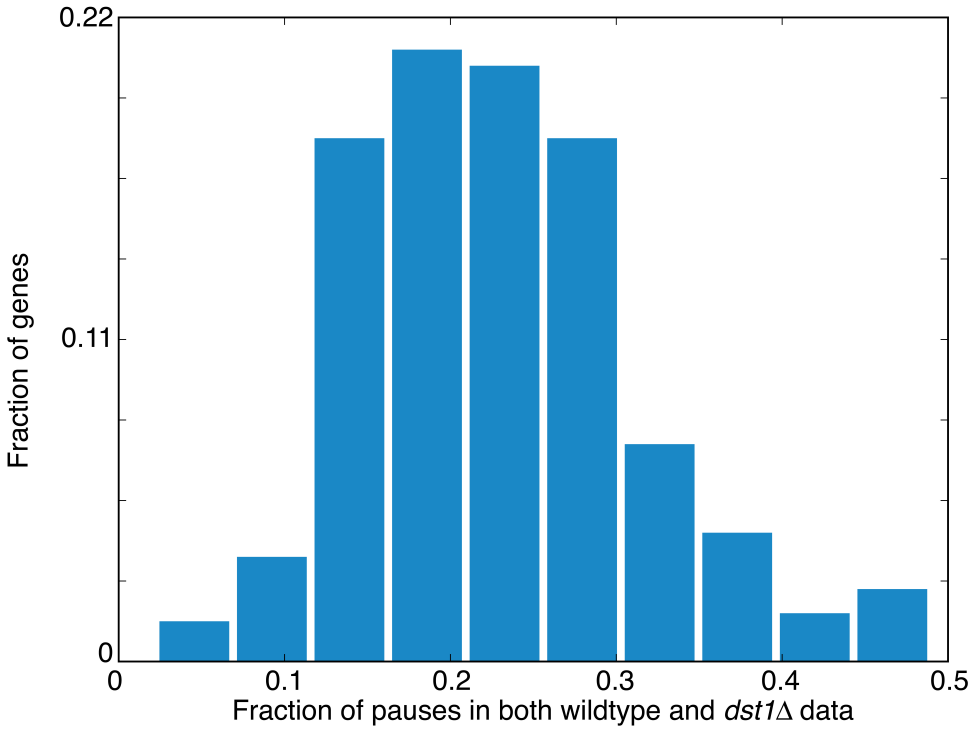

Supplementary Figure 8. Histogram of the fraction of pauses that are found in both wildtype *dst1Δ* data.

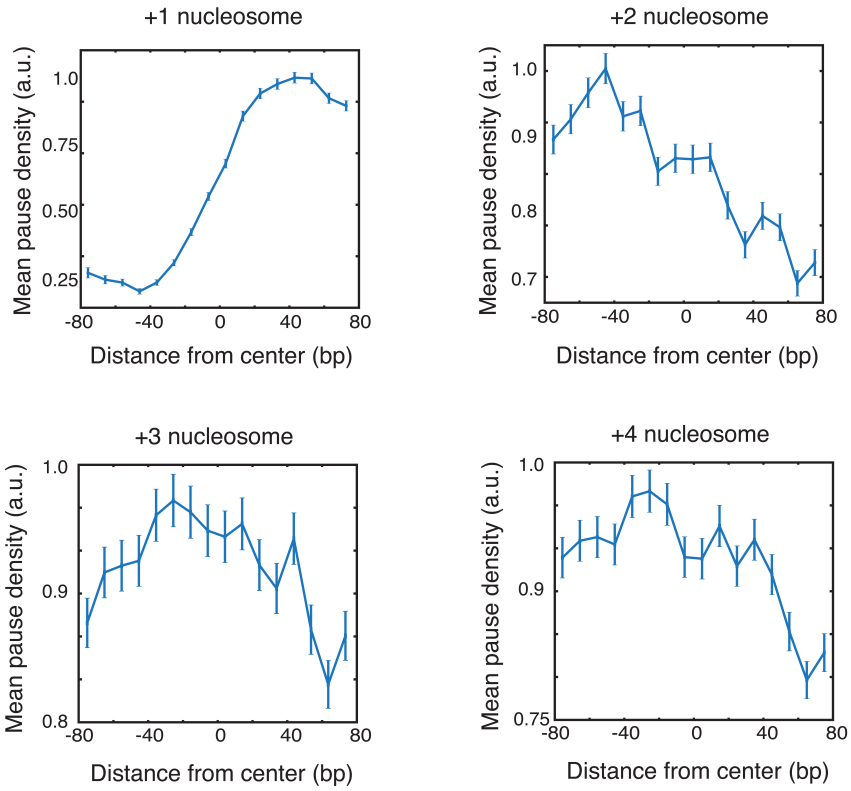

Supplementary Figure 9. Mean pause density of the wild type strain at the first four nucleosomes following transcription start sites. Error bars are placed at one standard deviation.

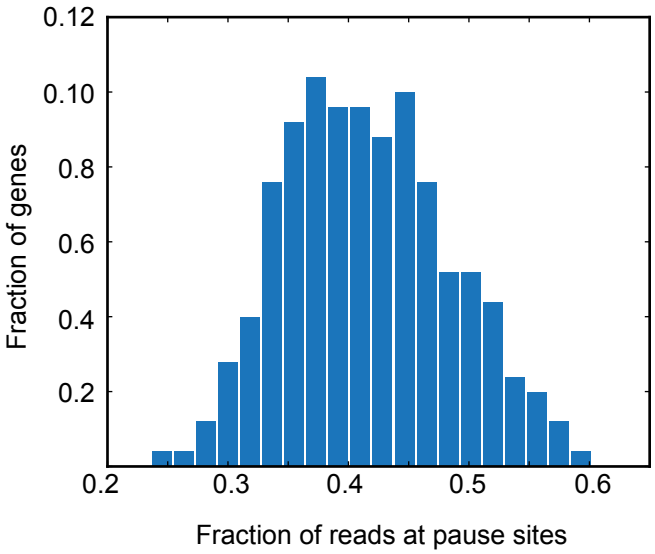

Supplementary Figure 10. Histogram of the fraction of reads at pause sites for highly-expressed genes (N = 256, >10 reads/bp). The reads at all pause sites was summed and then divided by the total number of reads for the gene resulting in the fraction of reads at pause sites.

Supplementary Methods

Western blot. Proteins were transferred from SDS–PAGE gels to nitrocellulose membranes and probed for FLAG-labelled proteins by using standard western blot procedures with rabbit anti-Flag (Sigma Aldrich). Western blots were scanned using an Odyssey fluorescent scanner (Li-Cor Biosciences).

qPCR analysis of the immunoprecipitation specificity. Strains expressing GFP did so by overexpression on a 2-micron plasmid from a pTEF2 promoter. ~100 ng of RNA eluted from the RNAP II immunoprecipitation (IP) was treated with DNAse I (Promega) according to the manufacturer's instructions. The GFP and TDH3 transcripts in the DNAse-treated RNA from the IP and the total RNA were converted to cDNA by reverse transcription using SuperScript III (Invitrogen) according to the manufacturer's instructions. GFP and TDH3 RT primers were 5' GTCATGCCGTTTCATATGATCTGGG and 5' GGGTCTCTTTCTTGGTAAGTAGCAATC respectively. qPCR reactions were set up using EXPRESS SYBR GreenER qPCR SuperMix Universal (Invitrogen) according to the manufacturer's instructions and for a series of cDNA template dilutions. TDH3 qPCR primers were 5' GTTGCTTTGAACGACCCATT and 5' GGGTCTCTTTCTTGGTAAGTAGCAATC. GFP qPCR primers were 5' CTGGAGTTGTCCCAATTCTTG and 5' GTTGGCCATGGAACAGGTAG. Detection of the PCR reaction was done by a continuous fluorescence detector (DNA Engine Opticon, MJ Research). Data analysis occurred as described[3], however, the differential amplification efficiencies of TDH3 and GFP were measured and accounted for.

Alignment	WT nascent 1		WT mRNA		WT nascent 2	
Total	51,174,644		51,079,222		6,935,019	
tRNA	1,225,423	2.39	162,182	0.32	138,477	2.00
rRNA	27,999,648	54.71	30,781,359	60.26	4,202,538	60.60
genomic	*19,395,914*	*37.90*	*17,653,868*	*34.56*	*1,877,403*	*27.07*

Alignment	WT nascent α-amanitin		Δrco1 nascent		Δdst1 nascent	
Total	12,105,338		18,796,881		29,652,801	
tRNA	137,260	1.13	600,024	3.19	933,844	3.15
rRNA	6,054,585	50.02	9,338,864	49.68	17,659,127	59.55
genomic	*5,175,283*	*42.75*	*7,812,384*	*41.56*	*9,588,097*	*32.33*

Supplementary Table 1. Alignment statistics. The total number of reads for each sample and the number of reads that align to tRNA, rRNA and genomic DNA followed by the percentage of each. With these statistics we estimated the amount of enrichment for nascent RNA that occurred during the RNAP II immunoprecipitation. Considering that the meadian lifetime of mRNA in yeast is 20 minutes[4], the expected concentration of nascent RNA is [nascent RNA]=(ln(2)/20) * [mature RNA]. As mRNA constitutes approximately 5% of the total RNA in a yeast cell[5], we expect nascent RNA to be 0.34% of the total RNA. Alignments to genomic regions represented 27%-42% of our total reads, thus the IP provided an approximately 100-fold enrichment for nascent RNA consistent with the direct measurement of enrichment made in our mixed lysate experiment (Supplementary Table 2).

	IP 1	IP 2
GFP (a.u.)	0.02	6.23
TDH3 (a.u.)	43.70	62.85
TDH3/GFP	0.00048	0.10
IP 1/IP 2	207.03	

Supplementary Table 2. Demonstration that IP conditions are strongly specific by two control IPs. The first IP used a mixed lysate of two strains: a strain endogenously expressing a FLAG-labelled Rpb3 and a strain expressing the wild type allele of Rpb3 and an ectopically expressed gene (GFP). The second IP was performed on lysate from a strain expressing both FLAG-labeled Rpb3 and GFP. qPCR on the RNA that co-purified from each IP (see Supplementary Methods) quantified the TDH3:GFP ratio which is summarized in the table. As the first IP had half the amount of labeled Rpb3 than the second IP, these results show that messages expressed in the same cells as a labeled Rpb3 are purified at least 100-fold more than messages from other cells.

Supplementary Note 1

References for Supplementary Information

1. Pokholok, D. K. *et al*. Genome-wide map of nucleosome acetylation and methylation in yeast. *Cell* **122**, 517-527 (2005).
2. Weiner, A., Hughes, A., Yassour, M., Rando, O. J. & Friedman, N. High-resolution nucleosome mapping reveals transcription-dependent promoter packaging. *Genome Res.* **20**, 90-100 (2010).
3. Livak, K. J. & Schmittgen, T. D. Analysis of relative gene expression data using real-time quantitative PCR and the 2(-Delta Delta C(T)) Method. *Methods* **25**, 402-408 (2001).
4. Wagner, A. Energy constraints on the evolution of gene expression. *Mol. Biol. Evol.* **22**, 1365-1374 (2005).
5. Warner, J. R. The economics of ribosome biosynthesis in yeast. *Trends Biochem. Sci.* **24**, 437-440 (1999).